# Palmprint and Face Biometrics for Person Authentication Using Color Images

**Oluwamuyiwa Quadri Akinpelu**

Submitted to the
Institute of Graduate Studies and Research
in partial fulfillment of the requirements for the degree of

Master of Science
in
Computer Engineering

Eastern Mediterranean University
August 2020
Gazimağusa, North Cyprus

Approval of the Institute of Graduate Studies and Research

Prof. Dr. Ali Hakan Ulusoy
Director

I certify that this thesis satisfies all the requirements as a thesis for the degree of Master of Science in Computer Engineering.

Prof. Dr. H. Işık Aybay
Chair, Department of Computer Engineering

We certify that we have read this thesis and that in our opinion it is fully adequate in scope and quality as a thesis for the degree of Master of Science in Computer Engineering.

Assoc. Prof. Dr. Önsen Toygar
Supervisor

Examining Committee

1. Assoc. Prof. Dr. Duygu Çelik Ertuğrul
2. Assoc. Prof. Dr. Önsen Toygar
3. Asst. Prof. Dr. Mehtap Köse Ulukök

# ABSTRACT

Multimodal biometric systems aim to improve the recognition accuracy by minimizing the limitations of unimodal systems. There exist many unimodal biometric traits used for person authentication such as face, iris, fingerprint, palmprint, voice, etc. In this thesis, a study on face and palmprint authentication using color images to construct an effective multimodal system is presented.

Face recognition has been studied extensively in the biometrics community. Color face recognition approaches also exist in the literature in the last decades. On the other hand, automated palmprint identification using palmprint images has been extensively studied in the literature. However, most of the palmprint identification approaches exploit the gray-level images and there has been very little efforts to improve the palmprint identification using color information. Therefore, the use of color information from palmprint and face images using RGB, YCbCr and HSV color space representations are studied in this thesis.

The experiments are conducted on publicly available color face and color palmprint databases. The results are presented on RGB, YCbCr and HSV color spaces. The effect of different color spaces on face and palmprint authentication is presented at the end of the thesis.

**Keywords:** Multimodal biometric systems, unimodal biometric traits, face biometrics, palmprint biometrics, color spaces, gray-level images.

# ÖZ

Çoklu biyometri sistemleri, tekli sistemlerin sınırlamalarını en aza indirerek tanıma doğruluğunu artırmayı amaçlamaktadır. Yüz, iris, parmak izi, avuçiçi, ses, vb. gibi kişi kimlik doğrulaması için kullanılan birçok tekli biyometrik özellik vardır. Bu tezde, etkili bir çoklu sistem oluşturmak için renkli görüntüler kullanılarak yüz ve avuçiçi kimlik doğrulaması üzerine bir çalışma sunulmaktadır.

Yüz tanıma, biyometri topluluğunda kapsamlı olarak incelenmiştir. Renkli yüz tanıma yaklaşımları da son yıllarda literatürde mevcuttur. Öte yandan, avuçiçi görüntüleri kullanılarak otomatik avuçiçi tanımlaması literatürde kapsamlı bir şekilde incelenmiştir. Ancak, avuçiçi tanıma yaklaşımlarının çoğu gri düzeyli renksiz görüntülerden yararlanır ve renk bilgilerini kullanarak avuçiçi tanımasını iyileştirmek için çok az çaba harcanmıştır. Bu nedenle, bu tezde avuçiçi ve yüz görüntülerindeki renk bilgileri RGB, YCbCr ve HSV renk uzayı gösterimleri kullanılarak incelenmiştir.

Deneyler halka açık renkli yüz ve renkli avuçiçi veritabanları üzerinde yapılmıştır. Sonuçlar RGB, YCbCr ve HSV renk uzay gösterimleri kullanılarak sunulmuştur. Farklı renk uzaylarının yüz ve avuçiçi kimlik doğrulaması üzerindeki etkisi tezin sonunda sunulmuştur.

**Anahtar Kelimeler**: Çoklu biyometrik sistemler, tekli biyometrik özellikler, yüz biyometrisi, avuçiçi biyometrisi, renk uzayları, gri düzey görüntüler.

# DEDICATION

I want to dedicate the research to all organizations and individual researchers that primarily work with biometric traits for various purpose like in the verification or identification process that is a main aspect of security control.

# ACKNOWLEDGMENT

Most importantly, I would like to thank God Almighty for giving me life and good health to reach this phase of my educational career. Without this favour, to accomplish this research work cannot been possible.

I also want to extend my unlimited acknowledgement to my supervisor Assoc. Prof. Dr. Önsen Toygar, who assisted me without any hesitation in all phase of this work, with a detailed and topnotch explanation of the task to be done.

I want to thank my parents and siblings who always checked up on me and gave me that extra motivation and words of encouragement that I needed during the entire work.

Finally, I want to thank the entire academic staff of the Computer Engineering department for the thought process I obtained from them, which I applied in various stage of this work.

# TABLE OF CONTENTS

# LIST OF TABLES

# LIST OF FIGURES

# LIST OF ABBREVIATIONS

| | |
|---|---|
| BSIF | Binarized Statistical Image Features |
| CCD | Charge-Coupled Device |
| COEP | College Of Engineering Pune |
| DFT | Discrete Fourier Transforms |
| FAR | False Acceptance Rate |
| FEI | Educational Foundation of Ignatius |
| FERET | Facial Recognition Technology |
| FLF | Feature-Level Fusion |
| FMR | False Match Rate |
| FRR | False Rejection Rate |
| GAR | Genuine Accept Rate |
| ICA | Independent Component Analysis |
| LBP | Local Binary Patterns |
| LPQ | Local Phase Quantization |
| PCA | Principal Component Analysis |
| STFT | Short Term Fourier Transform |
| SVM | Support Vector Machine |

# Chapter 1

# INTRODUCTION

In our society today, several factors need to be considered when addressing the issue of security control and person authentication. These issues can be solved easily with the use of a biometric system. It is utterly important to note that we use biometrics to carry out most of our daily activities. For this reason, the study of biometrics has been in the spotlight for more than a millennium. According to [1], the use of biometrics is primordial and the first biometric system was used far back in the 1800s when it was used for criminal classification and body measurements.

Even with the fact that more features were incorporated during the 19th and 20th century to enhance the existing system, there were still some minor setbacks. These hindrances led to a need to create more sophisticated and intelligent systems that made use of single biometric traits like face, iris, fingerprint, palmprint, etc.; to improve the system performance. The aforementioned systems that were created are known as “unimodal biometric systems”.

Not until the 21st century, unimodal biometric systems were in vogue and it was used for various purposes, but it seemed prone to mistake in some areas when the composition of the inputs to the system were complex. This setback led to the modelling of multimodal system, which helped to solve most of the problems in the unimodal biometric systems. Until now, most agencies and companies make use of the multimodal biometric system due to its ability to process high inflow of data gotten from a combination of more than one biometric trait.

## 1.1 What is a Biometric System?

Biometrics is a method of identifying humans with their behavioral or physiological traits that has had several focus in the last decade. It is related to the field of pattern recognition, which aims at taking into account different factors such as lines, segmentation and orientations of the target-object. A biometric system is a system that allows the recognition of a certain characteristic of an individual using mathematical algorithms and biometric data [2]. Some major qualities that a biometric modality should possess are acceptability (the use of the biometric modality should be accepted by the users), measurability (ease in obtaining and weighing samples), uniqueness (each feature from a particular subject should be a distinct attribute), performance (a versatile and efficient modality), permanence (consistency in the biometric trait), etc.

Over the years, the usage of an automated process for identifying humans has been a major discussion in various sectors such as e-commerce, security control at the airports and border control. Token-based systems and knowledge-based systems such as smart cards and passwords respectively were initially used to facilitate the verification and identification process in those sectors. Unfortunately, there were some setbacks with such systems because they can easily get stolen, lost or duplicated. Thus, with the use of such aforementioned systems, the issue of security that the system has to deliver keeps arising. To overcome most of these issues, the use of a system that dwells on biometric traits was used to replace the former systems because the latter system can never be lost or stolen.

A standard biometric system can be represented as a flow of actions where the successor task makes use of the inputs gotten from the predecessor task to generate the best possible output. Such flow of work is shown in Figure 1.1 [3].

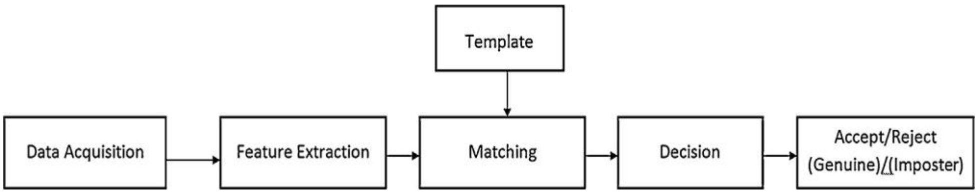


Figure 1.1: A typical biometric authentication system [3]

### 1.1.1 Unimodal Biometric Systems

In unimodal biometric systems, a single trait such as palmprint or face is used for the purpose of deciding if a person is genuine or an impostor to the system. This type of system is very common because it is used in human daily activities. An example of the use of a unimodal mode of recognition is in the use of thumbprints to gain access to a smartphone. A unimodal biometric system is based on a single trait, thus, it has some defects such as spoof attacks, and others stated in [4].

Various sceneries can be considered when trying to model a unimodal system but a very common scenery is with the use of a dataset containing various samples of the same type of biometric trait. In various organizations with large number of workers having different facial orientation, skin color, ethnicity, age and gender, it is always difficult to differentiate workers easily. Fortunately, this problem can be solved with the use of a unimodal biometric system that is primarily used for identifying respective individuals with the use of their biometric trait. An instance of a trait is in the use of palmprint for recognition just as it was done in this research. This process of identification can be accomplished by using a probe image to seek for a possible match from a repository containing trained facial images. A detailed explanation of how the matching process was done is presented later in Chapter 5. The illustration of a unimodal system workflow with the use of palmprint is shown in Figure 1.2 [5].

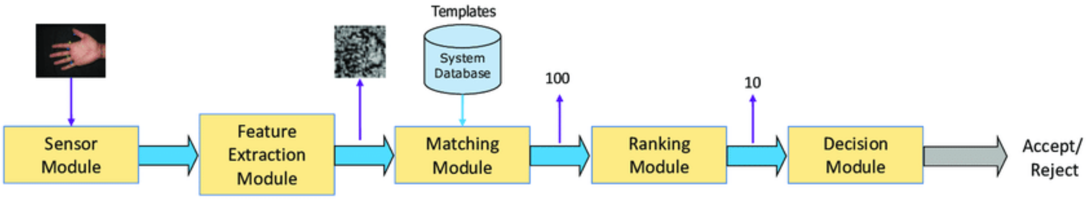


Figure 1.2: General block diagram of a unimodal biometric system [5]

An important issue that needs to be taken into consideration is the limitation to the unimodal biometric system. For instance, a biometric sensor can be vulnerable to poor formation of the data gotten from a biometric trait. This is a common problem when using palmprint for recognition just like in the case of a genuine user being identified as an impostor to the system due to a cut obtained on one of the principal lines on the palm. According to [6], a major limitation of the unimodal system is that unimodal biometrics are prone to inter-class similarities within a large population. All of these limitations tend to reduce the overall system accuracy when using single biometric traits.

In terms of the implementation cost, a unimodal system is cheaper than most other types of biometric system. In regards to this, most firms prefer to make use of this type of system but an ideal motive should be to improve the general system performance of a biometric system. For this reason, it is known that a biometric system in a multimodal mode is more efficient than a unimodal system. This type of system that works with the combination of multiple biometric traits is presented in the following section.

### 1.1.2 Multimodal Biometric System

A multimodal biometric system is a compositional system that combines two or more biometric automation such as palmprint, facial recognition, speech recognition, fingerprint, etc. This type of system takes its input from a sensor for measuring a combination of different biometric property. For example, any system combining face and palmprint characteristics for the purpose of identification is considered as a multimodal biometric system even if different imaging device or sensors captured the biometric traits. The system can be used for verifying or rejecting users with the help of the modality used as an input to the system. Figure 1.3 [3] shows how multiple biometric data are transferred from one unit to another unit in a multimodal biometric system until it reaches the final stage of verification.

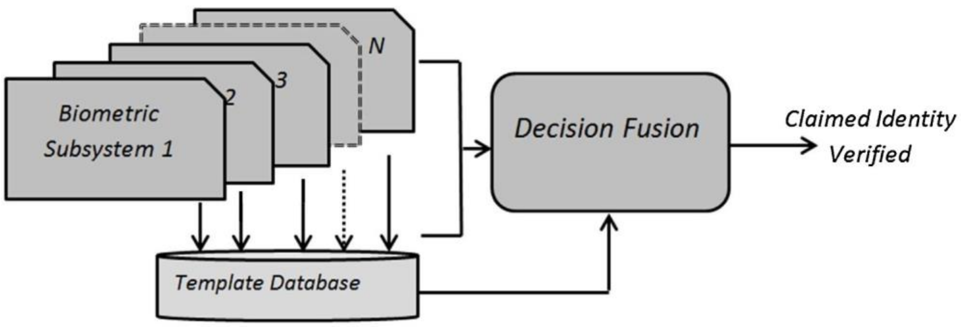


Figure 1.3: Flow of data in a multimodal biometric system [3]

In this work, the proposed system focuses on the multimodal mode with the use of features extracted from the face and the palmprint. This system works with a fusion-based method where two or more biometric traits against different algorithms are used to obtain a final decision. This method is very essential in cases where there is a large scale of users in the system that needs to be authenticated simultaneously. A major advantage of using the multimodal system is that there is always an extra trait to be used if one existing trait in the system malfunctions or gives an illogical result. With respect to the fact that this system helps to solve the limitations encountered in the unimodal system, corporations and public sectors in the financial firms and medical field makes use of the multimodal biometric system as their main system for recognizing and granting access to their staff.

The multimodal system comprises of four main modules, which are as follows: sensor module, feature extraction module, matching module and decision-making module. Figure 1.4 [7] shows how these modules are connected with one or more relationships between them.

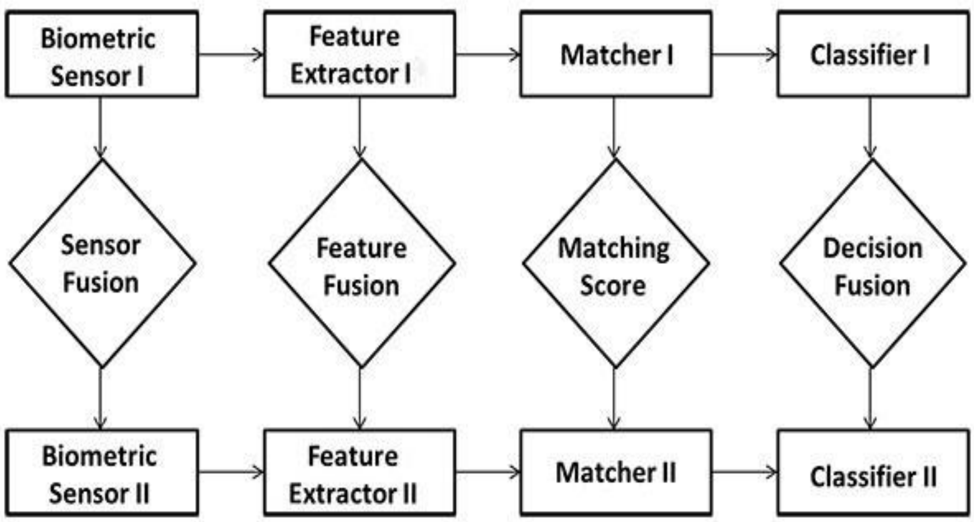


Figure 1.4: Fusion levels in multimodal biometric system [7]

## 1.2 Problem Statement

Over the period where unimodal biometric systems were used as the main frontier to gain access to the systems in corporate establishments, there have always been issues of intruders trying to breach into the system. Biometric companies are aware of these flaws in the technology and should aim to improve identification. There are some ways to deter inherent downfalls of biometrics like requiring more than one fingerprint scan to improve accuracy [8].

Furthermore, there have been reported cases where unimodal biometric systems have been compromised. Another problem with the system is in the issue of intra-user variations and inter-class similarities when using it for facial recognition. All of these have created a major setback to the use of biometric systems. Unfortunately, a feel of uncertainty have been developed in the mind of users as to if their information remains confidential and inaccessible by third parties.

In relation to these entire problems, questions may arise from potential users of the system. Some of these questions by users may vary from “Is my identity safe” to “How efficient is a multimodal system be over a unimodal system”. The technical expertise on how to solve these issues has been one of the major challenge to most biometric companies and it has gotten a great deal of public attention for more than a decade.

The implementation of a system that can make use of several biometric modality to grant or deny access to a system becomes very essential. In this thesis, some local texture descriptors were used for the extraction of features, which aided in finding the best match for a probe image in a range of trained images. The experiments were conducted using two face and two palmprint datasets. In Chapter 5, a further discourse on the datasets used in this thesis is presented. At the end, a comparison between the system proposed in this thesis and the state-of-the-art systems in terms of performance for person authentication is presented.

## 1.3 Applications of Biometric Systems

Biometrics plays a vital role in human daily activities ranging from online transactions to security control. It has gained a massive popularity because the protocols involved in most of biometrics mechanism is easy to use for everyone. Some of the common areas where biometrics are mainly used are in the governmental (healthcare, airport, border control) and commercial (smartphones, banking and finance) sector. Biometric technology can help to facilitate the process involved in border control protocols that helps in keeping the borders safe from illegal migrants. Additionally, doctors can access medical records of all patients in a hospital with the use of their physiological or behavioral biometric traits. Other applications of biometrics include employee-related usage for checking their attendance and monitoring the time an employee gets in and goes out of work.

## 1.4 Expected Outcome of the Study

An extensive study has been done in relation to the comparison between the unimodal and multimodal systems. As one may assume, the multimodal system should mostly likely have the upper hand over unimodal systems. Some of the areas that experts can foretell that the multimodal system is more superior is in the area of security regulation, accuracy, cost-effectiveness, universality, etc.

In addition, it can be predicted that when the influx of data to the system increases exponentially, the unimodal biometric system might experience some lag when making use of individual color channels from either of RGB, YCbCr, or HSV color space. The reason for the previously mentioned setback is because the unimodal mode makes use of only one trait and there is a high probability that some area of a particular biometric trait such as the face may be altered due to noise or illumination conditions.

Unlike unimodal systems, there is always an extra biometric trait (e.g. addition of palmprint to the face images) in multimodal systems to help solve this issue. Thus, the multimodal system studied has a better performance and higher accuracy for the authentication of users to the system when using color images.

## 1.5 The Work Done in this Study

The main objective of this thesis was to authenticate a user of a system with the combination of facial and palmprint features. A pair of database containing facial and palmprint images were used for training and testing purpose. Various experiments with different parameters were conducted using the features obtained from the aforementioned biometric traits. In this work, three different color spaces, which are RGB, YCbCr and HSV, were used. Each of these color spaces was further separated into 3 channels (e.g. R, G and B individual channels in the RGB color space) in order to test for the most suitable working condition with respect to possible change in illumination.

Some feature extraction techniques were used to get valuable information about a user of the system to know if the input he/she stored during the acquisition and registration phase is the same as the input that is currently being used by the user to access the system. The feature extraction methods used in this thesis are PCA (Principal Component Analysis), LBP (Local Binary Pattern), LPQ (Local Phase Quantization) and BSIF (Binarized Statistical Image Features), which are described in Chapter 3. The features extracted are trained using some mathematical model, after which the trained features of a specific subject are reshaped. A final step is the use of distance scores to check for features with minimum distance, after which the matching was done.

The rest of the thesis is organized as follows. The literature review and an in-depth discussion of multimodal systems are explained in Chapter 2. In Chapter 3, the feature extraction methods used are detailed with their methodology. The proposed method and architecture of the system are presented in Chapter 4. Chapter 5 focuses on the experimental analysis and results obtained in this work. Finally, conclusion and deductions are presented in Chapter 6.

# Chapter 2

# LITERATURE REVIEW

## 2.1 Introduction

In a multimodal system, an appropriate decision and a better classification of data are obtained when the data points are placed appropriately to obtain distinctive information about each trait. This is because a multimodal biometric system uses at least two biometric modalities for fusion. With the use of the fusion mechanism, there is a more flexible and low amount of defective data in the system. A typical multimodal biometric system is more reliable because it has a hierarchical nature, which implies that a user trying to gain access to the system has to pass through multiple levels of authentication that invariably requires two or more traits in some cases. The issue of non-universality that has been pointed out in most literatures can be resolved with the examination and separation of patterns from various biometric modalities. A major advantage of this type of system is that a user can still be granted access to the system even when there is a false rejection or loss of pattern in some modalities. In contrary to this, there have also been some disadvantages of using the multimodal biometrics system. Some challenges with the system are multimodal biometric systems are difficult to design [9], user acceptance is quite low [10], it requires higher level of investment [11] and the performance tradeoff [11].

As discussed in Chapter 1, a biometric modality possesses some major qualities such as uniqueness, permanence, etc. An in-depth review has been made regarding these qualities in relation to some biometric traits. Table 2.1 [12] shows the comparison of various biometric traits with the performance level.

Table 2.1: Comparison of Biometric Traits [12] (G: good, B: bad, G/B: indecisive)

| **BIOMETRICS** | **UNIVERSALITY** | **UNIQUENESS** | **PERMANENCE** | **MEASURABILITY** | **PERFORMANCE** | **ACCEPTABILITY** | **CIRCUMVENTION** |
|---|---|---|---|---|---|---|---|
| **FACE** | G | G/B | B | G | G/B | G | G |
| **FINGERPRINT** | B | G | G | B | G | B | B |
| **HAND GEOMETRY** | B | B | B | G | B | B | B |
| **IRIS** | G | G | G | B | G | G/B | G/B |
| **RETINA** | G | G | B | G/B | G | G/B | G/B |
| **VOICE** | B | G/B | G/B | B | G/B | G | G |
| **EAR** | G | G | B | G | G | G | G |
| **SIGNATURE** | G/B | G/B | G/B | G/B | G/B | B | B |
| **DNA** | B | B | B | B | B | G/B | G/B |
| **KEYSTROKE** | G/B | G/B | G/B | G/B | G/B | G | G |

From Table 2.1, it is seen that physiological and behavioral characteristics such as face and signature respectively were used for the comparison purpose. G signifies that the biometric trait possess good characteristic when used with the factors listed column-wise, B represents bad characteristic, and G/B stands for an indecisive characteristics (neither good nor bad) for the criteria. According to [13], the biometrics that can be relied upon are face, fingerprint and ear.

## 2.2 Previous Work Done on Multimodal Systems

From previous research carried out on unimodal systems, it has been observed that there have been an occurrence of many problems either in the preliminary stage such as image acquisition, or in one phase of the system functionality. However, the multimodal systems have helped to solve some problems in the unimodal system related to spoof attacks and high false match rates.

In relation to the proposed system, other studies and propositions have been made regarding the use of multimodal biometric systems. Some other strategies made by other researchers in the field of biometrics are also in vogue, but as we know, there is always a need to improve some state-of-the-art methodologies. A good instance of a previous work done stated that multi-biometric systems have two basic categories: synchronous and asynchronous. In synchronous, two or more biometrics combined within a single authorization process. On the other hand, asynchronous system uses two biometric technologies in sequence (one after the other) [14][15].

Sentosa et.al in [13] and [16] made a study on an important subject in biometrics. Face, fingerprint and finger-vein were the biometric traits used in their study. SVM-based score level fusion was used and they join all the three traits for the verification phase. A higher accuracy of mean GAR of 0.999 and a mean FAR of $3x10^7$ were obtained due to the fusion based on SVM classifiers.

Similarly, a study on face and palmprint was done by Gayatri et.al [17] where a feature level fusion system using a simple fusion algorithm was proposed. An accuracy of

81.48% was obtained using palm images only. The GAR using face images has an overall performance of 88.88%.  The fusion results of the face and palm images indicate a significant increase in the system to be 95%, FAR of 0.5%, and FRR of 1.2%.

# Chapter 3

# FEATURE EXTRACTION

## 3.1 Definition of Feature Extraction

In this chapter, the major discussion studied is on the methods that were applied to get distinct set of features from an image in a given color space. In most biometric systems, the initial input image to the system may be in an untidy or irregular form, and this makes it very difficult to identify the user accurately. For this reason, it is an ideal practice during the experimental phase to preprocess the input image before any other process.

One of the most important steps in the preprocessing stage is the feature extraction. Before any further discussion on feature extraction, it is important to understand what a feature represents in image preprocessing. A feature is a piece of information that is relevant for solving the computational task related to a certain application [18]. An appropriate description of a feature can be thought of as lines, corners or objects, which creates a flow in image sequences. A feature is one of the major framework in the development of a meaningful representation of a trait sample. Thus, it is important to assemble features, extract useful details out of it and use the details to create a disparity between all the candidate features in the system to get an optimal solution in the decision-making process.

In a study by Mohan et.al [19], feature extraction is a dimensionality reduction process, where an initial set of raw variables is reduced to more manageable groups (features) for processing, while still accurately and completely describing the original data set. In the field of biometrics and image processing, there are different types of feature extraction techniques with varying mode of operation and functionalities. In this research work, the techniques that were discussed are PCA, LBP, LPQ and BSIF. An illustration of how these techniques work is presented in the next section.

Figure 3.1 [20] shows the processes that are involved in the feature extraction stage in a feed-forward systematic flow. The first stage is the acquisition of a probe image, after which some other preprocessing techniques are done on the image before the actual feature extraction. In some cases such as in the use of PCA, there is a high focus on the dimensionality reduction factors, which plays a vital role in the recognition phase.

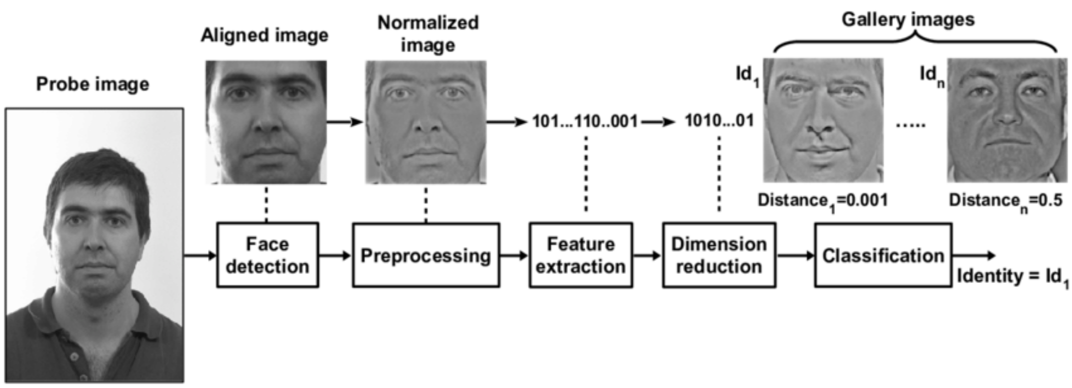


Figure 3.1: A general local feature-based facial recognition framework [20]

## 3.2 Implementation of the Feature Extraction Methods

In this section, a detailed discourse on the feature extraction methods that were used in this research work is highlighted. Each of the methods have their respective functionalities, which would be given in details. Although, some methods are slightly similar to each other just as in the case of local texture descriptors such as LBP, LPQ and BSIF. Another method that is studied is the PCA technique that is mainly used for dimensionality reduction.

### 3.2.1 Principal Component Analysis

Principal Component Analysis is a very common method in image processing and pattern recognition. It has various functionalities and it uses various parameters such as eigenvectors, eigenvalues, standard deviation and covariance to carry out its task. PCA can be used for either interpretation or data reduction, however, in this research work; it is used for the purpose of interpretation (finding out important features in a bulky dataset).

In the research studies presented by [21] and [22], PCA is defined as an orthogonal linear transformation that transforms the data to a new coordinate system. The greatest variance by some scalar projection of the data comes to lie on the first coordinate (called the first principal component), the second greatest variance on the second coordinate, and so on. Figure 3.2 [23] shows a graphical representation of the direction of the principal component. In order to achieve an optimal output using a PCA algorithm, some steps must be carried out.

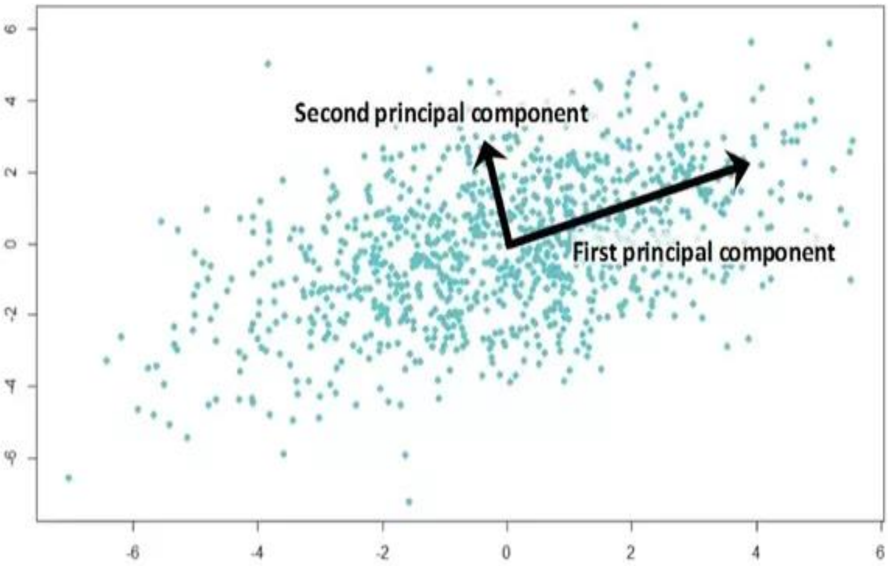


Figure 3.2: Components of PCA [23]

The first step in a typical PCA algorithm is to standardize the dataset. The following step is to find the covariance matrix like in equation (3.1) with the use of a sample mean, total candidate features and data points in the set. Covariance matrix is calculated as:

$$\mathrm{C} = \mathrm{X}^{\mathrm{T}}\mathrm{X} \tag{3.1}$$

where **C** is the covariance matrix, **X** is the data matrix and **T** is the transpose.

After this step, it is necessary to obtain the eigenvectors and eigenvalues with respect to the covariance matrix as follows:

$$\mathrm{CE} = \mathrm{VE} \tag{3.2}$$

where **E** is the eigenvector and **V** is the eigenvalue.

The next procedure is to map respective eigenvalues to their corresponding eigenvectors. Furthermore, it is a common practice to form an eigenvector matrix with the selection of **k** eigenvalues. The final step is the transformation of the original matrix. When carrying out data reduction process, it is ideal to implement the previously mentioned steps.

On the other hand, the steps involved when PCA is used for interpreting images is slightly different with some additional terminologies. In this study, the first step in the interpretation phase was to apply histogram equalization and mean-variance normalization. After this operation, an average and the centered images in the dataset were obtained, in which the covariance matrix was calculated from the constructed images.

Additional steps include finding and sorting the Eigenvectors and Eigenvalues of the covariance matrix, obtaining the Eigen-faces of all images, and projecting images into the Eigen-space with sorted eigenvectors. Figure 3.3 [24] and Figure 3.4 [25] show a representation of Eigenfaces.

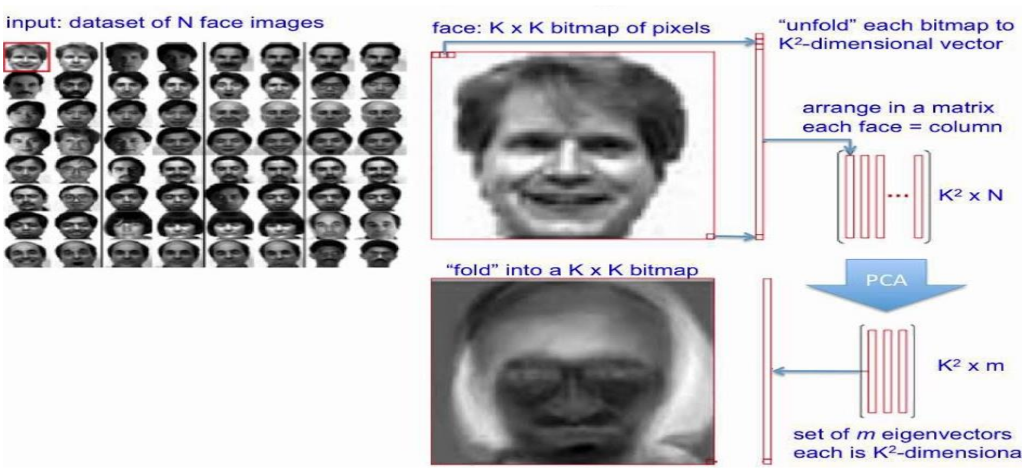


Figure 3.3: Extraction of Eigenfaces with PCA [24]

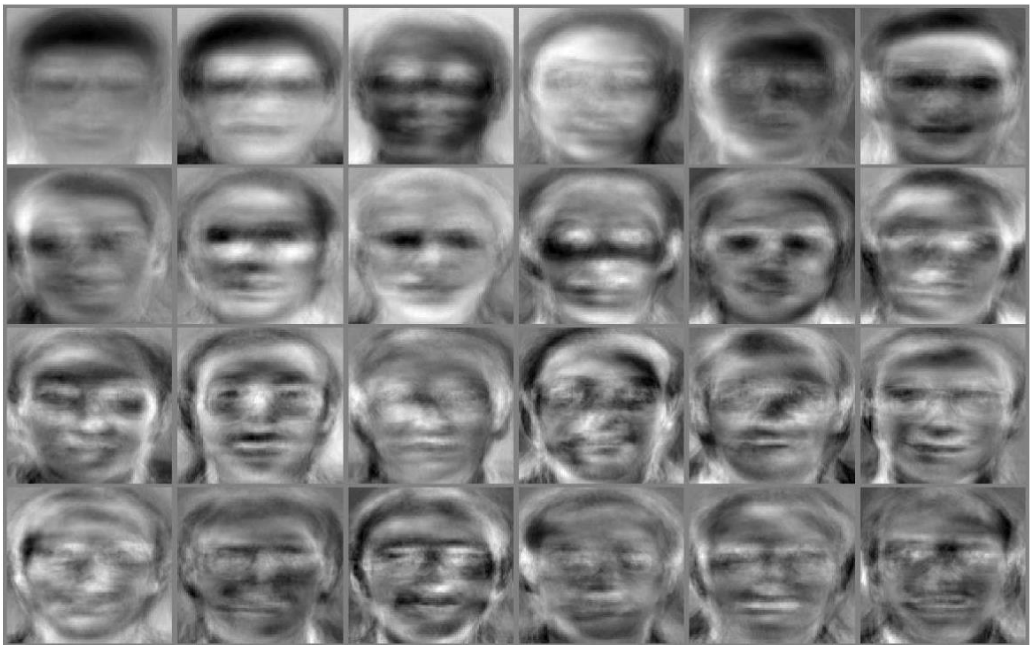

Figure 3.4: Dataset of Eigenfaces images [25]

### 3.2.2 Local Binary Patterns

The feedback from most researchers after using the LBP method has proven that the method yields a positive performance in most cases. The method has so many factors that maximizes the overall output of the features extracted using the method. Local Binary Pattern is a simple yet very efficient texture operator that labels the pixels of an image by thresholding the neighborhood of each pixel and considers the result as a binary number [26].

LBP texture descriptor operation is now a widely used method in most applications because of its computational clarity and discriminative power. In relation to the traditionally varying statistical and systematic models of texture description, it can be seen as an integrative approach.

One of the most important characteristics of the LBP method that makes it outstanding when compared to most feature extraction methods is its ability to withstand disadvantageous conditions like a change in the monotonic grayscales, which is mainly caused by an imbalance in the illumination factors. Furthermore, an additional important property that the LBP methods possess is the computational simplicity that supports the process of examining images in demanding real-time situations.

The steps involved in the LBP method are easy and undemanding. It mainly divides the original face image into segments, taking into account local details that makes from each subdivisions. Just as it is in Figure 3.5 [27], histograms are obtained from each subdivision and a feature histogram is finally obtained for further processing.

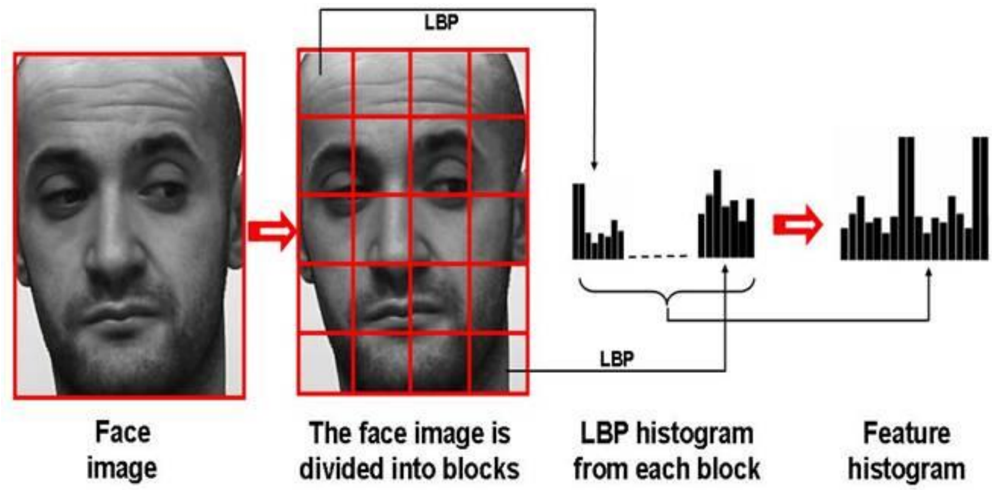


Figure 3.5: Face description with Local Binary Patterns [27]

In addition to the aforementioned steps, a mathematical computation to obtain the LBP-central pixel code of each cells is necessary. Equation (3.3) and (3.4) show the techniques involved in the calculation.

$$\text{LBP } (P_x, P_y) \sum_{p=0}^{p-1} S(P-C) \text{ x } 2^p \qquad (3.3)$$

where **P** is the neighboring pixel's intensity with index p, **C** is the central pixel's intensity, **p** is the number of sampling points, and **S** is the threshold step function, which is given as:

$$S(x) = \begin{cases} 1, & x \geq 0 \\ 0, & x < 0 \end{cases} \tag{3.4}$$

An example of the LBP calculation with a 3x3-neighborhood region is shown in Figure 3.6 [28].

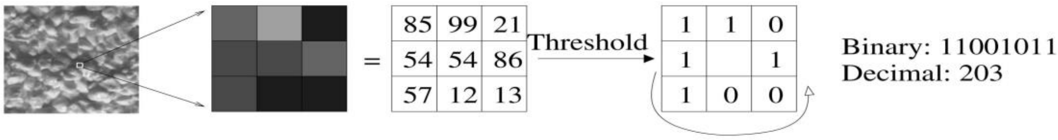


Figure 3.6: Example of a LBP code calculation [28]

### 3.2.3 Local Phase Quantization

The LPQ method is similar to the LBP method because they are both texture descriptors but there are some slight difference in the computation of the two approaches. The actual motive of using the LPQ was to outperform the LBP when processing images affected by blurs, noise or irregular illumination conditions. The LPQ is a method that was originally proposed by Ojansivu et.al [29] who stated that, it is based on the obscure invariance characteristics of the Fourier phase spectrum. LPQ extracts useful details at the local phase level using a 2-D short-term Fourier transform (STFT) calculated based on a rectangular neighborhood at each pixel position of the given image. Figure 3.7 [30] gives an illustration of the LPQ computational method. The "|" symbol in Figure 3.7 helps to differentiate the real from the imaginary part in the LPQ code calculation of a given central pixel.

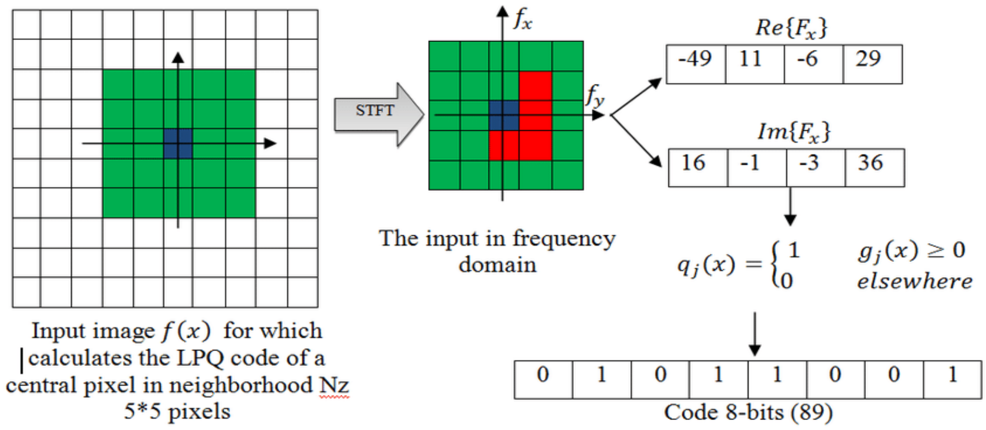


Figure 3.7: Example of a LPQ code calculation [30]

In LPQ method, it is known that the consideration of the parameters to be used is mainly focused on only four complex coefficients, which corresponds to 2-D frequencies. The coefficients are $u_1 = [a, 0]^T$, $u_2 = [0, a]^T$, $u_3 = [a, a]^T$, and $u_4 = [a, -a]^T$, where **a** is a scalar frequency.

A mathematical representation of the LPQ calculation is given in equation (3.5).

$$F(u,x) = \sum_{y \in N_x} f(x-y) e^{-j2\pi u^T y} = w_u^T f_x \tag{3.5}$$

where $\mathbf{w_u}$ is at frequency **u** signifying the basis vector of the 2-D DFT, and $\mathbf{f_x}$ is a vector that comprises of a sample of images. From equation (3.5), it can be noticed that a logical way of applying the STFT is to make use of 2-D convolutions $f(x) * e^{-2\pi jxu\wedge(T)}$ for all **u**. With the fact that the basis functions are separable, it can be proposed that with the use of 1-D convolutions for the rows and columns, the computations can be done.

### 3.2.4 Binarized Statistical Image Features

The BSIF method was specifically created for the use of comparisons with other texture descriptor methods. The baseline methods that were used for comparison with the BSIF method are texture classification techniques like LBP and LPQ method. Given a main set of small-scale natural images, the objective of the BSIF method is to spontaneously discover a static set of filters from the main set, rather than with the use of manual filters just as it is done in LBP and LPQ.

To obtain statistically significant characterization of the images, BSIF replaces the popular method of manual tuning with the method of learning from instances. This new approach enables a reliable information cryptography with the help of a quantization method that computes individual elements step-by-step. The issue of adjusting the descriptor length and its adaptability to sceneries with irregular image characterization can be done in an easy and adaptable way with the use of learning.

The intuition behind the BSIF method is the computation of a binary code that represents a given image's pixel. The steps involved in BSIF is discussed next. In a given pixel's neighborhood, a pixel's code value is regarded as a local descriptor of the image intensity pattern; the pixels are further represented as histograms with some code values that permit the characterization of texture features within the sub-regions of the image. This process consequently allows the BSIF method to be used in texture recognition systems in an akin way as in the LBP method. The next step is to set a threshold of zero, which is useful as a reference for computing the respective bits in the binary code string by changing the response of a linear filter to either black or white.

A different filter is mapped to each bit, and the number of filter **l** to be used is determined by the required length **n** of the bit string. A training set containing natural image blotch is useful for the learning process that is done by applying an incremental factor on the statistical independence of the response from the filters [31]. Thus, statistical traits of natural image blotches regulate the descriptors and they are known as "Binarized Statistical Image Features (BSIF)". A brief discussion on the details of learning the linear filters [31] is given below:

If part of an image with size ***l x l pixels*** and a linear filter $W_i$ have the same size, we obtain a filter response $S_i$ with the following equation:

$$S_i = XW_i\,(u,v)X(u,v) = w_i^T x \tag{3.6}$$

where parameters like **w** and **x** are the vector notations which are presented in the latter stage, and these parameters comprise of the pixels of $W_i$ and X. In some cases, there is a need to acquire a functional set of filters $W_i$, so it is a normal practice to apply the ideas of [31] and approximate the filters by the application of an incremental factor on the statistical independence of $S_i$.

BSIF descriptor has two aforementioned parameters, which are the length ***n*** of the bit string and the filter size ***l***. An example of a learnt filter size obtained with ***l***=9 and ***n***=8 is shown in Figure 3.8 [32].

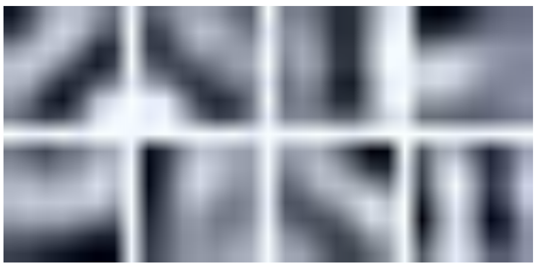

Figure 3.8: BSIF Learnt filters of size 9 x 9 [32]

Nevertheless, one needs to disintegrate the filter matrix **W** into two parts for making use of the benchmark ICA algorithms for estimating the independent component as follows:

$$S = Wx = UVx = Uz \tag{3.7}$$

where W is decomposed into UV, and z is also decomposed into Vx, whereby U is a **n x n** square matrix that is approximated with the use of ICA, and V is a matrix that does the canonical preliminary processing (whitening and the reduction of dimensions of the training samples **x** at the same time) [31].

In most facial recognition problems, the probe images contain a high amount of variations in illumination, facial expression, and fades. Some examples and the corresponding BSIF code images are shown in Figure 3.9 [32], where the classification is implemented with the use of the Nearest Neighbor Classifier.

Figure 3.9: A sample image, two probe images, and the BSIF codes [32]

According to a study by Kannala et.al [32], it was stated that the BSIF descriptor has a high tolerance to image deterioration that is a common problem in real-life applications.

# Chapter 4

# PROPOSED METHOD

## 4.1 Workflow and Architecture of the Proposed Method

This chapter is mainly going to focus on the proposed system of this research work. The multi-biometric system proposed is based on the combination of two biometric modalities namely face biometrics and palmprint biometrics. Figure 4.1 describes the architecture of the proposed system.

In a definition by [33], a biometric system architecture is the representation of a system as a single unit, where hardware and software components are mapped onto the components, the hardware architecture mapped onto the software architecture, and the interaction of humans with the mentioned components.

The proposed multimodal biometric system has all the functional units a unimodal system possess such as the image acquisition unit, feature extraction unit, comparison unit and decision making/classification unit. In addition to these units, it has some extra functionalities such as the fusion techniques that is mainly used for combining the data obtained from two distinct authentication systems. In the proposed system, the fusion of features can be performed at any of the following stage: (I) in the course of feature extraction, (II) during the comparison of the probe image with the images stored in the database, (III) in the course of the decision making/classification.

In this research, face and palmprint color images were used during the entire process of the experiments. The initial work done was with unimodal biometric traits like face or palmprint, where features from these traits were extracted. On the other hand, in the case where it was used in the application of a multimodal biometric trait, the face and palmprint images were fused together as a single processing unit, for the entire process of recognition. In both unimodal and multimodal systems, color images in the RGB, HSV and YCbCr color space were used. An additional step involving the separation of the color space into individual color channels (e.g. R, G and B individual channels from RGB color space) was carried out; this was primarily to solve the challenges that occurs in real-life applications such as variation in illumination condition of the images. The Manhattan distance score was used for the comparison of the test and trained image features of the facial and palmprint images.

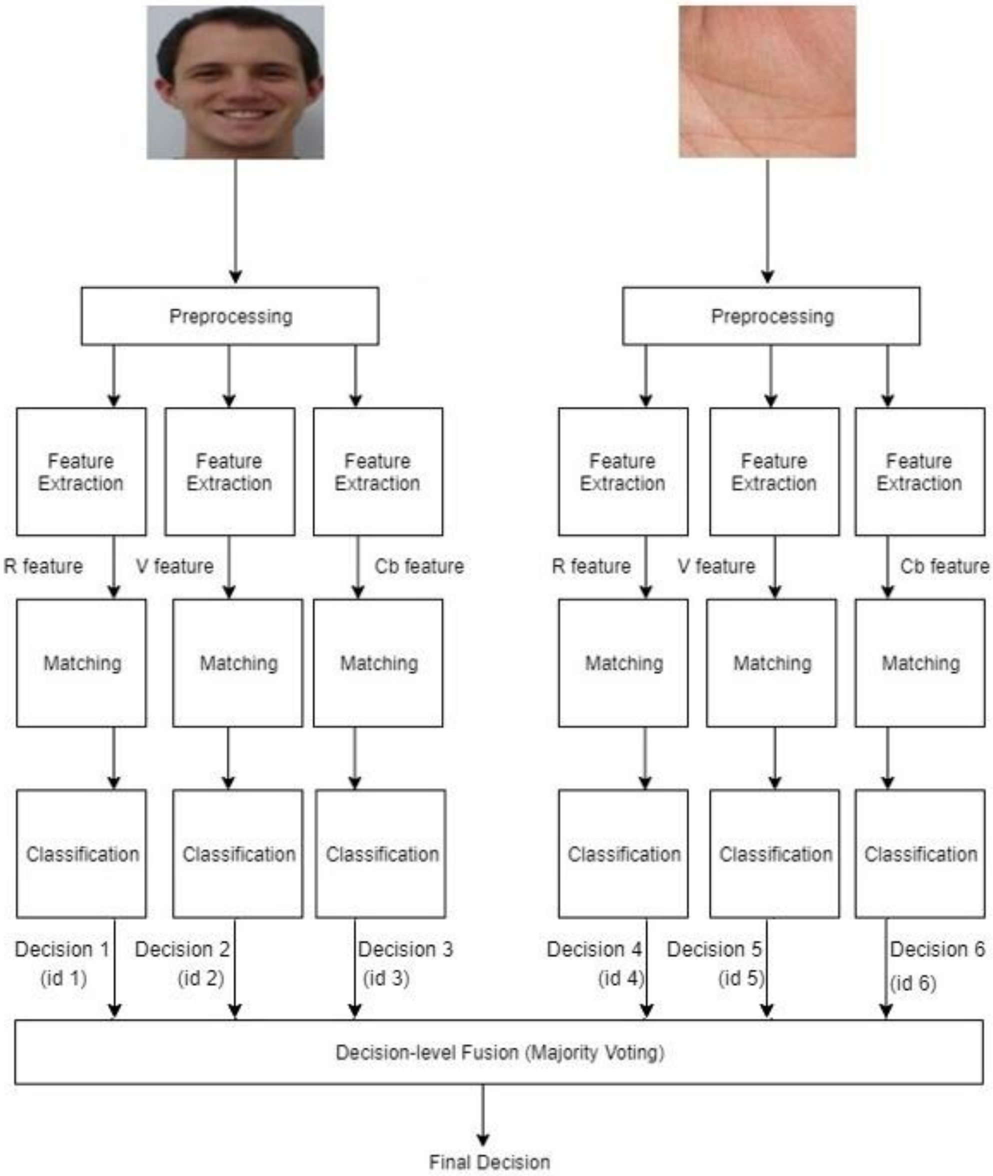


Figure 4.1: Proposed multi-biometric system architecture

## 4.2 Components of the Proposed Method

The proposed multi-biometric system is composed of five interconnected levels with the flow of data starting from the input/sensor level down to the decision level. The levels in the proposed system in an ascending order are as follows: preprocessing level, feature extraction level, matching level, classification level and the fusion level.

The first level is the preprocessing level, which mainly takes in the input from the sensors and helps with some further computational methods that help to make the biometric modalities unique. In the preprocessing level of this system, the MVN (Mean-and-Variance Normalization) technique was used as the standard method to preprocess the inputs. After preprocessing, the next stage is the flow of data to the second level. The feature extraction level is the second stage, and the LPQ (Local Phase Quantization) which is a popular texture descriptor method was used for the extraction of R, V and Cb features. The third level is the matching level and the Manhattan distance was used to check for the training image with the minimum distance from the probe image, which simply represents the most resembling trained image to the probe image. The fourth level primarily focused on the process of classification with the application of the Nearest Neighbor Classification technique that gives a parallel output decision to the next (decision-level) layer. The fifth level is the decision-level fusion layer that gets six distinct decisions from the face (three decisions) and palmprint (three decisions) system which has their respective IDs. This layer makes use of the Majority Voting methodology to obtain the final decision of the proposed system.

# Chapter 5

# EXPERIMENTS AND RESULTS

## 5.1 Introduction

In this chapter, the details of the datasets used are introduced. In addition, some preliminary work done is studied; after which there is a further discussions on the experimental setup, and the main points that can be observed from the experimental results.

## 5.2 Databases Used

This research had two main biometric traits (face and palmprint) so the database that were used in this work consists of two main categories which are face datasets and palmprint datasets. During the task of the facial recognition, the color FERET [34] and the FEI [35] datasets were used, while the Tongji Contactless palmprint dataset [36] and the COEP palmprint [37] database were used for the palmprint recognition.

### 5.2.1 ColorFERET Database

The ColorFERET database is one of the face databases that was used in this research. It consists of color images of 268 subjects having 2 samples each. As we know, in real-life applications, most of the data that is gotten from the input interface such as the sensors are generally obtained in the color format. Furthermore, the respective samples of each subject were captured in different tilts, pose and facial expression in order to test for varying state of the user's input. Figure 5.1 [34] shows a sample image from the ColorFERET dataset.

Figure 5.1: ColorFERET same face image with different facial expression [34]

### 5.2.2 FEI Face Database

FEI database is mainly composed of color images. It is a Brazilian face database formed by the Artificial Intelligence Laboratory of the FEI in Brazil. In total, there are 2800 images, with 200 subjects and 14 samples each. It has an equal number of male and female subjects taken at different pose. An analysis of how it was used in this work is presented in the following sections. Figure 5.2 [35] shows a sample image from the FEI dataset.

Figure 5.2: FEI same face image with different facial expression [35]

### 5.2.3 Tongji Contactless Palmprint Database

The Tongji Contactless Palmprint database is a very popular database for palmprint recognition due to its suitability for taking specific details on the region of interest in a palm image such as the thenar, distal palmar and proximal palmar. In this database, there are 1000 images comprising of 100 subjects with 10 samples each. Figure 5.3 [36] shows a sample image from the Tongji Contactless Palmprint dataset.

Figure 5.3: Sample ROI of Tongji Contactless palmprint image [36]

### 5.2.4 COEP Palmprint Database

The COEP palmprint database comprises of colored images in RGB color space. It is also a widely used database due to its diversity in usage to accomplish both hand recognition and palmprint recognition related problems. In this database, there are 1344 images of 168 individuals. Each of these individuals has 8 different images each of a single palm. Figure 5.4 [37] shows a sample image from the COEP palmprint dataset.

Figure 5.4: Sample ROI of COEP palmprint image [37]

## 5.3 Preliminary Experiments

In the implementation phase of the thesis, some experiments were conducted before the main work of the proposed system that focuses on multimodal recognition. The preliminary was done using color image of the FERET database that consisted of 1000 images, with 250 subjects having 4 samples each. The dataset was divided into 2 equal halves of training and testing images comprising of 500 images each. Furthermore, the feature extraction methods discussed in Chapter 3 were implemented on the grayscale images to extract features for the purpose of recognition and the final decision. The results obtained in the preliminary experiment are discussed in Section 5.5.

## 5.4 Experimental Setup

The experiments that were conducted in this research were divided into two similar categories with different datasets. The setups during the experiment focused on face and palmprint images. More details of the division of the database to form datasets are presented in Subsections 5.4.1 and 5.4.2.

### 5.4.1 Experimental Setup I

The first setup had two datasets that were created from the selection of a specific number of images. These image samples were acquired from the face and palmprint databases that were mainly used in this thesis. **D1** is the notation to identify the first dataset created, and **D2** represents the second dataset created. Both **D1** and **D2** were regarded as virtual datasets. **D1** was formed with images from the Tongji palmprint database and the FEI face database. From both database, a unique number of 100 subjects with 2 samples were taken respectively to form **D1.**

Another dataset that was formed is **D2,** which was formed using 100 subjects with 2 samples also from the Tongji palmprint database and the ColorFERET database. All the images were in the **RGB** color space initially, but they were transformed to other color spaces such as **YCbCr** and **HSV** for the purpose of comparison as to the most suitable method for person identification, verification and authentication.

An important factor is the dimension of the respective images for the recognition process. For the Tongji palmprint images, the dimension was 150x150 pixels in .bmp format. The face images datasets, which are the FEI and the ColorFERET, had dimensions of 260x360 pixels in .jpg format and 769x512 pixels in .ppm format, respectively.

### 5.4.2 Experimental Setup II

This setup is slightly similar to the Experimental Setup I with only a slight difference in the palmprint image that was used for the experiments. The setup also comprised of two datasets that were selected from the COEP, ColorFERET and FEI database. These image samples were acquired from the face and palmprint databases that were mainly used in this thesis. **D3** is the notation to identify the first dataset created in the Experimental Setup II, and **D4** is used to identify the second datasets created. Both **D3** and **D4** were regarded as virtual datasets. **D3** was formed with images from the COEP palmprint database and the ColorFERET face database. From both database, a unique number of 100 subjects with 2 samples were taken respectively and this was regarded as dataset **D3.**

Additionally, another dataset that was formed is **D4,** which was formed using 100 subjects with 2 samples each from the COEP palmprint database and the Color FEI face database. The images were also in the **RGB** color space just as it was in the experimental setup I, but were further mapped to **HSV** and **YCbCr** color space. The dimensions of the respective images that were used for the recognition process were 1600x1200 pixels in .jpg format for the COEP palmprint datasets. The face images datasets, which are the FEI and the ColorFERET, had dimensions of 260x360 pixels in .jpg format and 769x512 pixels in .ppm format, respectively.

Table 5.1: Contents of all datasets used

| Datasets | Face Dataset | Palmprint Dataset | Number of subjects | Number of samples | Experimental Setup |
|---|---|---|---|---|---|
| **D1** | Tongji | FEI | 100 | 2 | I |
| **D2** | Tongji | ColorFERET | 100 | 2 | I |
| **D3** | COEP | ColorFERET | 100 | 2 | II |
| **D4** | COEP | FEI | 100 | 2 | II |

For both Experimental Setups (I and II), the steps taken during the implementation of the system are given below:

**Step 1:** After splitting the datasets into two equal halves, the top half is used for training purpose and the bottom half is used for testing. The top half images (training images) are read from the device with the use of a loop and they are stored on a local cache to make them inaccessible by other systems.

**Step 2:** After all the images have been read, all stored images are retrieved from the cache and the colored images are converted to grayscale images in some cases.

**Step 3: P**reprocessing to the images are applied to obtain the local features that is necessary for acquiring important details of respective images. A widely used method namely MVN (Mean-and-Variance Normalization) is applied to the images in this stage.

**Step 4:** In this stage, it is important to apply any of the feature extraction technique that was mentioned in Chapter 3 depending on the type of task. There is a need to reshape the various sub-cells gotten after the use of texture descriptors like LBP and LPQ. This is useful because these type of methods work by partitioning the entire image into equal number of rows and columns (e.g. 3x3 or 5x5 partitioning).

**Step 5:** The next step is to read the test images, which represents the bottom half samples of each subject. The same procedures that were done in **step 1 to 4** are repeated for the test images.

**Step 6:** After a successful completion of Step 5, a probe image from the test set is taken as the subject of focus. For recognition purpose, it is necessary to apply a distance metric such as the **Manhattan distance** to check for the training image with the minimum distance from the probe image, which represents the most resembling images to the probe image.

**Step 7:** The total number of test images that was correctly matched is stored into a variable that keeps the count of the total number of accurate matches.

**Step 8:** The final step is to calculate the overall accuracy of the system with the use of the following formula to determine if the user is accepted or rejected into the system as follows:

$$Accuracy\ (\%) = \frac{\text{Number of test images correctly classified}}{\text{Total number of test images}}\ x\ 100 \qquad (5.1)$$

Finally, there were four main phases for both experimental setups but this thesis is mainly going to focus on the results gotten from the final stage, which is related to the multimodal recognition using color images. The stage of the experiments for both setups are as follows:

**Phase 1 (RGB to Grayscale):** This is the first category of experiments that was carried out. For both experimental setups, the face and palmprint datasets were used with the feature extraction methods to get specific features. All the images were converted from RGB color space to a grayscale before extracting those features. Some further preprocessing techniques were done depending on the type of feature extraction method being used. The final stage of this phase is the classification and final decision making as the output.

**Phase 2 (Channel separation):** This phase of the experiment dwells on the decomposition of the color space used in this work. It primarily splits each color space into their respective individual channels before the application of the feature extraction methods. For instance, the HSV color space is split into H (Hue) channel, S (Saturation) channel and V (Value) channel. A typical scenario in this phase is working on a face or palmprint dataset, reading the images, extracting any of the three channels in the RGB, HSV or YCbCr color space and applying one of the feature extraction method. The final stage is the decision-making stage where the user is either accepted or rejected.

**Phase 3 (FLF):** In this phase, the main components are the data gotten at the feature level. The process involved in the FLF phase is similar to that of the Channel separation phase with some additional steps. The additional steps involved in this phase is the concatenation of the features gotten. For example, if there is a need to apply FLF on an image in the RGB color space, the first step is to separate the respective R (Red), G (Green) and B (Blue) channels into their individual color planes; after which there is a concatenation process to fuse the features acquired from the three channels. The feature vector normalization is an important step that should be done just before the fusion of the biometric traits. The fused features act as a single unit for further processing like the matching and final decision. A block diagram of the FLF implementation was shown in Chapter 4.

**Phase 4 (FLF + Multimodal recognition):** This phase is the main area of interest in this study. It uses a combination of the results gotten from the three aforementioned phases, and the concatenation of the actual face and palmprint traits. Just like in the case of a unimodal system where only a face, iris or palmprint trait is used for the recognition purpose, it has the same application in the multimodal system where the concatenated face and palmprint traits are used for the same purpose like it was done in this research. This very useful phase solves biometric related issues such as spoof attacks/identity theft. The next subsection is going to cover the findings and experimental results obtained during each experimental setup.

## 5.5 Experimental Results and Discussion

This section is mainly going to report all the results obtained in the two experimental setups (Experimental Setups I and II). Preliminary experiments on gray images of the FERET dataset are demonstrated in Table 5.2 using PCA, LBP, LPQ and BSIF feature extraction methods to show the performance of each method on gray images. The total images for the preliminary experiments are 1000 grayscale images, in which the dataset was divided into 500 training images and 500 testing images.

Table 5.2: Results of the preliminary experiments

| Method | Accuracy (%) |
|---|---|
| PCA | 92.8 |
| LBP | 96 |
| LPQ | 96.8 |
| BSIF | 91.4 |

From the results obtained in preliminary experiments, it can be observed that LPQ had the best performance with 96.8% followed by LBP, which are both texture descriptor methods. The least performance was with the BSIF and PCA methods. In subsequent experiments, there is mainly going to be a focus on the texture descriptor methods such as LBP, LPQ and BSIF method.

Afterwards, the results from Experimental Setup I are demonstrated in Table 5.3 for unimodal face and palmprint datasets used for Dataset 1 and Dataset 2. The results are obtained by converting RGB images into grayscale images.

Table 5.3: Unimodal Palmprint and Face results on Grayscale Images

| | **Method** | | | |
|---|---|---|---|---|
| **Palmprint and Face Datasets** | **PCA** | **LBP** | **LPQ** | **BSIF** |
| Tongji Palmprint (D1) | 86% | 99% | 98% | 82% |
| FEI Face (D1) | 73% | 73% | 73% | 69% |
| Tongji Palmprint (D2) | 69% | 99% | 99% | 66% |
| ColorFERET Face (D2) | 90% | 99% | 97% | 96% |

In the next experimental stage, the results were based on the separation of the RBG, HSV and YCbCr color space into individual color channels. In addition, a feature-level fusion was implemented on the individual channels gotten from color space. Table 5.4 and Table 5.5 shows the results obtained with the application of the aforementioned method using the RGB color space on Dataset 1 and Dataset 2 respectively.

Table 5.4: FLF results on RGB color space on Dataset 1

| | **RGB Color space** | | | |
|---|---|---|---|---|
| **Dataset 1 Method** | **R** | **G** | **B** | **FLF (R+G+B)** |
| **LBP (Tongji Palmprint)** | 94% | 97% | 96% | 84% |
| **LPQ (Tongji Palmprint)** | 97% | 91% | 95% | 85% |
| **BSIF (Tongji Palmprint)** | 72% | 80% | 80% | 70% |
| **LBP (FEI Face)** | 67% | 65% | 61% | 80% |
| **LPQ (FEI Face)** | 74% | 72% | 69% | 92% |
| **BSIF (FEI Face)** | 68% | 70% | 73% | 75% |

Table 5.5: FLF results on RGB color space on Dataset 2

| | **RGB Color space** | | | |
|---|---|---|---|---|
| **Dataset 2 Method** | **R** | **G** | **B** | **FLF (R+G+B)** |
| **LBP (Tongji Palmprint)** | 94% | 97% | 98% | 61% |
| **LPQ (Tongji Palmprint)** | 96% | 99% | 97% | 62% |
| **BSIF (Tongji Palmprint)** | 49% | 61% | 56% | 58% |
| **LBP (ColorFERET Face)** | 98% | 98% | 98% | 62% |
| **LPQ (ColorFERET Face)** | 98% | 98% | 98% | 70% |
| **BSIF (ColorFERET Face)** | 94% | 96% | 96% | 66% |

The result obtained during the application of feature-level fusion on RBG color space shows that the best result was obtained in Dataset 2 with the use of the **LPQ** algorithm on the **G** channel.

Furthermore, Table 5.6 and Table 5.7 shows the results obtained with the application of the feature-level fusion using the YCbCr color space on Dataset 1 and Dataset 2.

Table 5.6: FLF results on YCbCr color space on Dataset 1

| | **YCbCr Color space** | | | |
|---|---|---|---|---|
| **Dataset 1 Method** | **Y** | **Cb** | **Cr** | **FLF (Y+Cb+Cr)** |
| **LBP (Tongji Palmprint)** | 95% | 88% | 87% | 83% |
| **LPQ (Tongji Palmprint)** | 95% | 92% | 92% | 82% |
| **BSIF (Tongji Palmprint)** | 74% | 68% | 79% | 76% |
| **LBP (FEI Face)** | 64% | 60% | 52% | 80% |
| **LPQ (FEI Face)** | 73% | 76% | 64% | 93% |
| **BSIF (FEI Face)** | 71% | 63% | 63% | 81% |

Table 5.7: FLF results on YCbCr color space on Dataset 2

| | **YCbCr Color space** | | | |
|---|---|---|---|---|
| **Dataset 2 Method** | **Y** | **Cb** | **Cr** | **FLF (Y+Cb+Cr)** |
| **LBP (Tongji Palmprint)** | 94% | 86% | 75% | 60% |
| **LPQ (Tongji Palmprint)** | 96% | 93% | 86% | 57% |
| **BSIF (Tongji Palmprint)** | 77% | 69% | 77% | 71% |
| **LBP (ColorFERET Face)** | 98% | 98% | 86% | 62% |
| **LPQ (ColorFERET Face)** | 97% | 97% | 97% | 74% |
| **BSIF (ColorFERET Face)** | 85% | 78% | 90% | 70% |

The result obtained during the application of feature-level fusion on YCbCr color space shows that the best result can be observed in Dataset 2 with the use of the **LBP** algorithm on the **Y** and **Cb** channel.

Table 5.8 and Table 5.9 shows the results obtained with the application of the feature-level fusion using the HSV color space on Dataset 1 and Dataset 2.

Table 5.8: FLF results on HSV color space on Dataset 1

| | **HSV Color space** | | | |
|---|---|---|---|---|
| **Dataset 1 Method** | **H** | **S** | **V** | **FLF (H+S+V)** |
| **LBP (Tongji Palmprint)** | 94% | 92% | 96% | 84% |
| **LPQ (Tongji Palmprint)** | 94% | 90% | 96% | 84% |
| **BSIF (Tongji Palmprint)** | 96% | 100% | 81% | 90% |
| **LBP (FEI Face)** | 65% | 67% | 69% | 80% |
| **LPQ (FEI Face)** | 70% | 70% | 70% | 92% |
| **BSIF (FEI Face)** | 61% | 70% | 69% | 88% |

Table 5.9: FLF results on HSV color space on Dataset 2

| | **HSV Color space** | | | |
|---|---|---|---|---|
| **Dataset 2 Method** | **H** | **S** | **V** | **FLF (H+S+V)** |
| **LBP (Tongji Palmprint)** | 91% | 90% | 98% | 61% |
| **LPQ (Tongji Palmprint)** | 92% | 82% | 100% | 60% |
| **BSIF (Tongji Palmprint)** | 96% | 98% | 66% | 73% |
| **LBP (ColorFERET Face)** | 98% | 99% | 99% | 62% |
| **LPQ (ColorFERET Face)** | 98% | 99% | 99% | 70% |
| **BSIF (ColorFERET Face)** | 95% | 96% | 97% | 85% |

The result obtained during the application of feature-level fusion on HSV color space shows many good results in both Dataset 1 and Dataset 2. It can be observed that the best result in Dataset 1 was with the use of the **BSIF** algorithm on the **S** channel. On the other hand, the best result in Dataset 2 was with the **LPQ** algorithm on the **V** channel.

The results reported in the next experimental stage is mainly on the use of multimodal biometric trait. The face and palmprint images from Dataset 1 and Dataset 2 were used for this purpose. Table 5.10, Table 5.11 and Table 5.12 shows the rate of accuracy on

RGB, HSV and YCbCr color space respectively on Dataset 1 with the proposed feature extraction methods.

Table 5.10: Multimodal recognition results on RGB color space on Dataset 1

| | **Multimodal Recognition Rate (%)** | | | |
|---|---|---|---|---|
| **Feature Extraction Method** | **R** | **G** | **B** | **R+G+B** |
| **LBP (Tongji Palmprint + FEI Face)** | 99% | 99% | 99% | 81% |
| **LPQ (Tongji Palmprint + FEI Face)** | 99% | 99% | 99% | 94% |
| **BSIF (Tongji Palmprint + FEI Face)** | 83% | 87% | 82% | 79% |

Table 5.11: Multimodal recognition results on HSV color space on Dataset 1

| | **Multimodal Recognition Rate (%)** | | | |
|---|---|---|---|---|
| **Feature Extraction Method** | **H** | **S** | **V** | **H+S+V** |
| **LBP (Tongji Palmprint + FEI Face)** | 98% | 96% | 99% | 77% |
| **LPQ (Tongji Palmprint + FEI Face)** | 98% | 97% | 99% | 93% |
| **BSIF (Tongji Palmprint + FEI Face)** | 80% | 97% | 82% | 78% |

Table 5.12: Multimodal recognition results on YCbCr color space on Dataset 1

| | **Multimodal Recognition Rate (%)** | | | |
|---|---|---|---|---|
| **Feature Extraction Method** | **Y** | **Cb** | **Cr** | **Y+Cb+Cr** |
| **LBP (Tongji Palmprint + FEI Face)** | 98% | 97% | 93% | 78% |
| **LPQ (Tongji Palmprint + FEI Face)** | 97% | 99% | 91% | 91% |
| **BSIF (Tongji Palmprint + FEI Face)** | 77% | 66% | 57% | 76% |

From the results obtained in the multimodal recognition stage on Dataset 1, there is a good performance in both LBP and LPQ method when comparing individual channels but the **LPQ** method was the best in the feature-level fusion and overall comparison.

Table 5.13, Table 5.14 and Table 5.15 shows the rate of accuracy on RGB, HSV and YCbCr color space respectively, with the proposed feature extraction methods on Dataset 2.

Table 5.13: Multimodal recognition results on RGB color space on Dataset 2

| | **Multimodal Recognition Rate (%)** | | | |
|---|---|---|---|---|
| **Feature Extraction Method** | **R** | **G** | **B** | **R+G+B** |
| **LBP (Tongji Palmprint + ColorFERET Face)** | 100% | 100% | 100% | 66% |
| **LPQ (Tongji Palmprint + ColorFERET Face)** | 100% | 100% | 100% | 83% |
| **BSIF (Tongji Palmprint + ColorFERET Face)** | 96% | 95% | 97% | 72% |

Table 5.14: Multimodal recognition results on HSV color space on Dataset 2

| | **Multimodal Recognition Rate (%)** | | | |
|---|---|---|---|---|
| **Feature Extraction Method** | **H** | **S** | **V** | **H+S+V** |
| **LBP (Tongji Palmprint + ColorFERET Face)** | 100% | 100% | 100% | 73% |
| **LPQ (Tongji Palmprint + ColorFERET Face)** | 100% | 100% | 100% | 81% |
| **BSIF (Tongji Palmprint + ColorFERET Face)** | 100% | 99% | 67% | 70% |

Table 5.15: Multimodal recognition results on YCbCr color space on Dataset 2

| | Multimodal Recognition Rate (%) | | | |
|---|---|---|---|---|
| **Feature Extraction Method** | **Y** | **Cb** | **Cr** | **Y+Cb+Cr** |
| **LBP (Tongji Palmprint + ColorFERET Face)** | 100% | 97% | 100% | 64% |
| **LPQ (Tongji Palmprint + ColorFERET Face)** | 100% | 100% | 99% | 79% |
| **BSIF (Tongji Palmprint + ColorFERET Face)** | 67% | 64% | 85% | 60% |

From the results obtained in the multimodal recognition stage on Dataset 2, **LPQ** method outperformed all other methods in the individual comparison and the feature-level fusion overall comparison.

In general, from the results obtained in the Experimental Setup I, the LPQ (Local Phase Quantization) had a better performance in the proposed multimodal biometric system with an average accuracy of **99%**.

The next results are from the Experimental Setup II. The results demonstrated in Table 5.16 for unimodal face and palmprint recognition on Dataset 3 and Dataset 4. The results are obtained by converting RGB images into grayscale images.

Table 5.16: Unimodal Palmprint and Face results on Grayscale Images with Dataset 3 and Dataset 4

| | Method | | | |
|---|---|---|---|---|
| **Palmprint and Face Datasets** | **PCA** | **LBP** | **LPQ** | **BSIF** |
| COEP Palmprint (D3) | 46% | 49% | 49% | 61% |
| ColorFERET Face (D3) | 74% | 75% | 75% | 59% |
| COEP Palmprint (D4) | 48% | 51% | 53% | 64% |
| FEI Face (D4) | 92% | 99% | 99% | 97% |

The results in the next experimental stage are based on the separation of the RBG, HSV and YCbCr color space into individual color channels. However, Table 5.17 and Table 5.18 shows the results obtained with the application of a feature-level fusion on the individual color channels obtained using the RGB color space on Dataset 3 and Dataset 4 respectively.

Table 5.17: FLF results on RGB color space on Dataset 3

| | **RGB Color space** | | | |
|---|---|---|---|---|
| **Dataset 3 Method** | **R** | **G** | **B** | **FLF (R+G+B)** |
| **LBP (COEP Palmprint)** | 50% | 47% | 49% | 60% |
| **LPQ (COEP Palmprint)** | 47% | 52% | 50% | 55% |
| **BSIF (COEP Palmprint)** | 61% | 65% | 60% | 61% |
| **LBP (ColorFERET Face)** | 69% | 67% | 62% | 68% |
| **LPQ (ColorFERET Face)** | 76% | 73% | 71% | 89% |
| **BSIF (ColorFERET Face)** | 66% | 69% | 71% | 62% |

Table 5.18: FLF results on RGB color space on Dataset 4

| | **RGB Color space** | | | |
|---|---|---|---|---|
| **Dataset 4 Method** | **R** | **G** | **B** | **FLF (R+G+ B)** |
| **LBP ( COEP Palmprint)** | 52% | 49% | 50% | 73% |
| **LPQ (COEP Palmprint)** | 51% | 53% | 51% | 64% |
| **BSIF (COEP Palmprint)** | 50% | 61% | 56% | 50% |
| **LBP (FEI Face)** | 99% | 99% | 99% | 51% |
| **LPQ (FEI Face)** | 99% | 98% | 98% | 77% |
| **BSIF (FEI Face)** | 92% | 94% | 95% | 55% |

The result obtained during the application of feature-level fusion on RBG color space shows that the best results were obtained in Dataset 4 with the use of the **LBP** and **LPQ** algorithm on the **R** channel.

Table 5.19 and Table 5.20 shows the results obtained with the application of the feature-level fusion using the YCbCr color space on Dataset 3 and Dataset 4.

Table 5.19: FLF results on YCbCr color space on Dataset 3

| | YCbCr Color space | | | |
|---|---|---|---|---|
| **Dataset 3 Method** | **Y** | **Cb** | **Cr** | **FLF (Y+Cb+Cr)** |
| **LBP (COEP Palmprint)** | 50% | 38% | 40% | 68% |
| **LPQ (COEP Palmprint)** | 50% | 50% | 48% | 61% |
| **BSIF (COEP Palmprint)** | 52% | 53% | 50% | 60% |
| **LBP (ColorFERET Face)** | 68% | 60% | 55% | 70% |
| **LPQ (ColorFERET Face)** | 75% | 76% | 64% | 91% |
| **BSIF (ColorFERET Face)** | 73% | 66% | 66% | 74% |

Table 5.20: FLF results on YCbCr color space on Dataset 4

| | YCbCr Color space | | | |
|---|---|---|---|---|
| **Dataset 4 Method** | **Y** | **Cb** | **Cr** | **FLF (Y+Cb+Cr)** |
| **LBP (COEP Palmprint)** | 53% | 41% | 41% | 67% |
| **LPQ (COEP Palmprint)** | 51% | 51% | 48% | 61% |
| **BSIF (COEP Palmprint)** | 50% | 59% | 50% | 60% |
| **LBP (FEI Face)** | 100% | 99% | 91% | 48% |
| **LPQ (FEI Face)** | 99% | 99% | 97% | 77% |
| **BSIF (FEI Face)** | 90% | 82% | 93% | 74% |

The result obtained during the application of feature-level fusion on RBG color space shows that the best result was obtained in Dataset 4 with the use of the **LBP** algorithm on the **Y** channel. The **LPQ** algorithm also had the best performance at the feature-level fusion with an accuracy of 77%.

Table 5.21 and Table 5.22 shows the results obtained with the application of the feature-level fusion using the HSV color space on Dataset 3 and Dataset 4.

Table 5.21: FLF results on HSV color space on Dataset 3

| | HSV Color space | | | |
|---|---|---|---|---|
| **Dataset 3 Method** | **H** | **S** | **V** | **FLF (H+S+V)** |
| **LBP (COEP Palmprint)** | 48% | 48% | 47% | 66% |
| **LPQ (COEP Palmprint)** | 39% | 48% | 49% | 63% |
| **BSIF (COEP Palmprint)** | 50% | 61% | 55% | 60% |
| **LBP (ColorFERET Face)** | 69% | 70% | 71% | 84% |
| **LPQ (ColorFERET Face)** | 72% | 72% | 73% | 95% |
| **BSIF (ColorFERET Face)** | 63% | 74% | 71% | 69% |

Table 5.22: FLF results on HSV color space on Dataset 4

| | HSV Color space | | | |
|---|---|---|---|---|
| **Dataset 4 Method** | **H** | **S** | **V** | **FLF (H+S+V)** |
| **LBP (COEP Palmprint)** | 48% | 51% | 50% | 69% |
| **LPQ (COEP Palmprint)** | 42% | 51% | 52% | 63% |
| **BSIF (COEP Palmprint)** | 48% | 60% | 56% | 60% |
| **LBP (FEI Face)** | 99% | 99% | 99% | 56% |
| **LPQ (FEI Face)** | 99% | 99% | 99% | 76% |
| **BSIF (FEI Face)** | 93% | 95% | 96% | 72% |

The result obtained during the application of feature-level fusion on RBG color space shows that the best result was obtained in Dataset 4 with the use of the **LPQ** algorithm on all **H, S** and **V** channel. The **LPQ** algorithm also had the best performance at the feature-level fusion.

The results reported in the next experimental stage is mainly on the use of multimodal biometric trait. The face and palmprint images from Dataset 3 and Dataset 4 were used for this purpose. Table 5.23, Table 5.24 and Table 5.25 shows the rate of accuracy on RGB, HSV and YCbCr color space respectively on Dataset 3 with the proposed feature extraction methods.

Table 5.23: Multimodal recognition results on RGB color space on Dataset 3

| | **Multimodal Recognition Rate (%)** | | | |
|---|---|---|---|---|
| **Feature Extraction Method** | **R** | **G** | **B** | **R+G+B** |
| **LBP (COEP Palmprint + ColorFERET Face)** | 58% | 46% | 40% | 68% |
| **LPQ (COEP Palmprint + ColorFERET Face)** | 53% | 69% | 73% | 85% |
| **BSIF (COEP Palmprint + ColorFERET Face)** | 65% | 62% | 67% | 60% |

Table 5.24: Multimodal recognition results on HSV color space on Dataset 3

| | **Multimodal Recognition Rate (%)** | | | |
|---|---|---|---|---|
| **Feature Extraction Method** | **H** | **S** | **V** | **H+S+V** |
| **LBP (COEP Palmprint + ColorFERET Face)** | 56% | 69% | 67% | 57% |
| **LPQ (COEP Palmprint + ColorFERET Face)** | 83% | 82% | 87% | 81% |
| **BSIF (COEP Palmprint + ColorFERET Face)** | 65% | 76% | 70% | 77% |

Table 5.25: Multimodal recognition results on YCbCr color space on Dataset 3

| | **Multimodal Recognition Rate (%)** | | | |
|---|---|---|---|---|
| **Feature Extraction Method** | **Y** | **Cb** | **Cr** | **Y+Cb+Cr** |
| **LBP (COEP Palmprint + ColorFERET Face)** | 66% | 60% | 64% | 76% |

| | | | | |
|---|---|---|---|---|
| **LPQ (COEP Palmprint + ColorFERET Face)** | 81% | 80% | 83% | 89% |
| **BSIF (COEP Palmprint + ColorFERET Face)** | 77% | 79% | 70% | 80% |

From the results obtained in the multimodal recognition stage on Dataset 3, **LPQ** method outperformed all other methods at the feature-level fusion with an accuracy of **85%, 81%,** and **89%** in the **RGB, HSV** and **YCbCr** color space.

Table 5.26, Table 5.27 and Table 5.28 shows the rate of accuracy on RGB, HSV and YCbCr color space respectively, with the proposed feature extraction methods on Dataset 4.

Table 5.26: Multimodal recognition results on RGB color space on Dataset 4

| | **Multimodal Recognition Rate (%)** | | | |
|---|---|---|---|---|
| **Feature Extraction Method** | **R** | **G** | **B** | **R+G+B** |
| **LBP (COEP Palmprint + FEI Face)** | 59% | 56% | 45% | 71% |
| **LPQ (COEP Palmprint + FEI Face)** | 71% | 81% | 77% | 88% |
| **BSIF (COEP Palmprint + FEI Face)** | 60% | 75% | 71% | 77% |

Table 5.27: Multimodal recognition results on HSV color space on Dataset 4

| | **Multimodal Recognition Rate (%)** | | | |
|---|---|---|---|---|
| **Feature Extraction Method** | **H** | **S** | **V** | **H+S+V** |
| **LBP (COEP Palmprint + FEI Face)** | 62% | 67% | 68% | 46% |
| **LPQ (COEP Palmprint + FEI Face)** | 83% | 81% | 87% | 72% |
| **BSIF (COEP Palmprint + FEI Face)** | 65% | 68% | 66% | 62% |

Table 5.28: Multimodal recognition results on YCbCr color space on Dataset 4

| | **Multimodal Recognition Rate (%)** | | | |
|---|---|---|---|---|
| **Feature Extraction Method** | **Y** | **Cb** | **Cr** | **Y+Cb+Cr** |
| **LBP (COEP Palmprint + FEI Face)** | 70% | 77% | 65% | 70% |
| **LPQ (COEP Palmprint + FEI Face)** | 89% | 84% | 84% | 84% |
| **BSIF (COEP Palmprint + FEI Face)** | 69% | 70% | 73% | 75% |

From the results obtained in the multimodal recognition stage on Dataset 3, **LPQ** method outperformed all other methods at the feature-level fusion with an accuracy of **88%, 72%,** and **84%** in the **RGB, HSV** and **YCbCr** color space.

In relation to the results from Experimental Setup II, it can be seen that the **LPQ** method had the best performance again when compared with the LBP and BSIF methods of the proposed multimodal biometric system. The LPQ methods had an overall average of **83%** with the Experimental Setup II.

Furthermore, from the results obtained in both experiments, it can be noted that the Experimental Setup I had an overall better performance than the Experimental Setup II.

The average computation times for all the feature extraction methods are given in Table 5.29.

Table 5.29: Average computation times for the feature extraction methods

| Method | Computation time (in seconds) |
|---|---|
| **PCA** | 137 |
| **LBP** | 240 |
| **LPQ** | 225 |
| **BSIF** | 71 |

The experiment was done using a Windows 10 professional Operating System with 4GB RAM and an Intel Core i5 CPU @ 2.60GHz.

The final step in the experimental phase is related to the application of a decision-level fusion on Dataset 1, Dataset 2, Dataset 3 and Dataset 4. In this phase, the biometric traits used are the face and palmprint modalities. Furthermore, the **R, V** and **Cb** channels were extracted from the **RBG, HSV** and **YCbCr** color space respectively. These extracted channels are proposed to be used in the system due to their performance in Experimental Setup I and Experimental Setup II. In addition, the feature extraction method that will be used in the proposed system is the LPQ method because it outperformed all other methods during the experiments conducted in Experimental Setups I and II. Table 5.30 shows the results obtained with the application of the LPQ feature extraction method and a decision-level fusion on the R, V and Cb color channels.

Table 5.30: Proposed Method (Decision-level fusion) results on Dataset 1 to Dataset 4

| | **Multimodal Recognition Rate (%)** | | | |
|---|---|---|---|---|
| **Datasets** | **R** | **V** | **Cb** | **Proposed Method (R+V+Cb)** |
| **Tongji Palmprint + FEI Face (D1)** | 98% | 99% | 94% | 96% |
| **Tongji Palmprint + ColorFERET Face (D2)** | 94% | 99% | 91% | 94% |
| **COEP Palmprint + ColorFERET Face (D3)** | 87% | 90% | 88% | 87% |
| **COEP Palmprint + FEI Face (D4)** | 89% | 86% | 89% | 90% |

From the results obtained, it can be observed that the best results were obtained in the use of **D1 (Dataset 1)** that is made up of the Tongji palmprint database and the FEI Face database. The color channel that had a generally better result than the others is the **V** channel with an accuracy of **99%** in D1 (Dataset 1) and D2 (Dataset 2).

Finally, a comparison between the preliminary experiments performed on the grayscale images and the experiments conducted on the color images for the proposed system can be made. It can be noted that the color images in the proposed system has an overall general performance in most of the phases that it was used in with high recognition rate in the R and V channels of RGB and HSV color spaces respectively. Although the best accuracy obtained as a single unit in the grayscale images using LPQ was 96.8%, it was slightly better than that of the color images in the proposed system of 96%. However, from the overall results obtained, it can be deduced that it is better to use color images for person authentication due to the extra features obtained from channel separation and fusion at various levels that give rich information related to each biometric trait.

# Chapter 6

# CONCLUSION

In this thesis, feature extraction algorithms such as Local Binary Patterns, Local Phase Quantization, Binarized Statistical Image Features and Principal Component Analysis were used on colored face and colored palmprint images that possessed various facial gesture and illumination conditions respectively to develop a system that is suitable for the authentication of a person using the mentioned biometric traits. Local Binary Patterns, Local Phase Quantization and Binarized Statistical Image Features were used as texture descriptors on the images to extract local histogram at all points of a sample with the use of some mathematical methods. The color compositions of the samples were taken into account while trying to distinguish certain properties of one feature from the other. The three distinct color spaces that were introduced in the proposed system are RGB, YCbCr and HSV color spaces. The proposed system in this thesis was mainly on the use of multimodal biometric system for person authentication using the color images of the biometric modalities that were fed into the system. The proposed system employs Decision-Level Fusion technique to combine six different decisions obtained using three different color spaces. In general, the proposed system has an encouraging performance compared to most of the existing systems that dwells on the use of multiple biometric traits for person authentication. The system is ready to be delivered to work sectors that uses computer vision and biometric systems to keep track of their employees and other identity-check process in the organization as this system is efficient enough due to its ability to process high influx of multiple biometric data simultaneously.

As a future work, the proposed system can be improved by adding some feature selection techniques to the existing feature extraction methods. The addition of this technique is useful in case of any alteration in the representation of the biometric data that may be caused due to some external factors or possible system malfunction.

# REFERENCES


[1] Jason, L. (2020). A Brief History of Biometrics. Retrieved from https://bioconnect.com/a-brief-history-of-biometrics/#:~:text=Where%20it%20Began,classification%20and%20comparison%20of%20criminals

[2] Souhail, G., Anass, M. & Ali, A. (2019, March 1). Biometric Systems and Their Applications [Online First], *IntechOpen*.

[3] Gopal, S.S., Saurabh, B., Sandeep, B. (2016). Fusion of palm-phalanges print with palmprint and dorsal hand vein. *Applied Soft Computing*, *47*, 12-20.

[4] Wang, K.Q., Khisa A.S., Wu X.Q., Zhao Q. (2012). Finger vein recognition using LBP variance with global. *2012 International Conference on Wavelet Analysis and Pattern Recognition (ICWAPR)*, 196–201.

[5] Kabir, W., Ahmad, M.O., Swamy, M.N. (2019). A Multi-Biometric System Based on Feature and Score Level Fusions. *IEEE Access*.

[6] Danny, T. (n.d). Unimodal Biometrics vs. Multimodal Biometrics. *Bayometric*. Retrieved from https://www.bayometric.com/unimodal-vs-multimodal/

[7] Srivastava, D.N. (2017). Fusion Levels in Multimodal Biometric Systems – A Review.

[8] Kevin, H. (2017). 3 Problems with Biometric security, including Fingerprint ID, Progress. Retrieved from https://blog.ipswitch.com/3-reasons-biometrics-are-not-secure#:~:text=Problem%20%233%3A%20Biometrics%20Hacks%20May,a%20stolen%20credit%20card%20number

[9] Oviatt, S., Cohen, P., Wu, L., Duncan, L., Suhm, B., Bers, J., Holzman, T., Winograd, T., Landay, J., & Larson, J. (2000). Designing the user interface for multimodal speech and pen-based gesture applications: state-of-the-art systems and future research directions. *Human-computer interaction*, *15(4)*, 263-322.

[10] Ribaric, S., Ribaric, D., & Pavesic, N. (2003). Multimodal biometric user-identification system for network-based applications. *IEE Proceedings-Vision, Image and Signal Processing*, *150(6)*, 409-416.

[11] Ross, A., & Jain, A.K. (2004). Multimodal biometrics: An overview. *Edition: Multimodal biometrics: An overview (IEEE, edn.)*, 1221- 1224.

[12] Arunarani, S., & Gobinath, R. (2018). Literature review on multimodal biometrics. *International Journal of Engineering & Technology*, 7*(2.26)*, 31-34.

[13] Arunarani, S., Gobinath, R. (2018). Literature review on multimodal biometrics. *International Journal of Engineering & Technology [Online]*, *7.2.26*, 31-34. Web. 8 Jul. 2020.

[14] Gad, R., El-Fishawy, N., El-Sayed, A., Zorkany, M. (2015). Multi-Biometric Systems: A State of the Art Survey and Research Directions. *International Journal of Advanced Computer Science and Applications*, *6*, 128-138.

[15] Deriche, M. (2008). Trends and Challenges in Mono and Multi biometrics. *Image Processing Theory, Tools and Applications*, *IPTA 2008*, 1-9.

[16] He, M., Horng, S.J., Fan, P., Run, R.S., Chen, R.J., Lai, J.L., Khan, M.K. & Sentosa K.O. (2010). Performance evaluation of score level fusion in multimodal biometric systems. *Pattern Recognition, 43(5)*, 1789-1800.

[17] Gayathri, U.B., Ashok M.S. (2012). Feature level fusion of palm and face for secure recognition. *International Journal of Computer and Electrical Engineering, 4(2).*

[18] Feature (computer vision). (n.d). Retrieved from https://en.wikipedia.org/wiki/Feature_(computer_vision)#:~:text=In%20computer%20vision%20and%20image,related%20to%20a%20certain%20application.&text=Features%20may%20be%20specific%20structures,as%20points%2C%20edges%20or%20objects

[19] Mohan, J., Kanagasabai, A., & Pandu, V. (2019). Real-Time ECG-Based Biometric Authentication System Countering Cyber Attacks and Preserving the Integrity and Availability of Critical Systems, *IGI Global,* 275-289.

[20] Nguyen, H. (2014). Contributions to facial feature extraction for face recognition.

[21] Jolliffe, I.T. (2002). Principal Component Analysis, Series: Springer Series in Statistics. *Springer, NY*, 28.

[22] Principal Component Analysis. (n.d). Retrieved from https://en.wikipedia.org/wiki/Principal_component_analysis#:~:text=PCA%20is%20defined%20as%20an,second%20coordinate%2C%20and%20so%20on

[23] PCA: A Practical Guide to Principal Component Analysis in R & Python. Retrieved from https://www.analyticsvidhya.com/blog/2016/03/pca-practical-guide-principal-component-analysis-python/

[24] PCA 10: Eigen faces. Retrieved from https://www.youtube.com/watch?v=_lY74pXWlS8

[25] Computer Vision Project 3: Eigen faces. Retrieved from https://courses.cs.washington.edu/courses/cse576/13sp/projects/project3/

[26] Matti, P. (2010). Local Binary Patterns. *Scholarpedia*, 5(3), 9775.

[27] Singh, S., Kaur, A., & Dir, T. (2015). A Face Recognition Technique using Local Binary Pattern Method. *International Journal of Advanced Research in Computer and Communication Engineering*, 165-168.

[28] Xia, W., Yin S., & Ouyang, P. (2013). A High Precision Feature Based on LBP and Gabor Theory for Face Recognition. *Sensors, 13(4)*, 4499-4513.

[29] Ojansivu, V., & Heikkila, J. (2008). Blur insensitive texture classification using local phase quantization. *ICISP*.

[30] Mebarka, B., Meriem, L., Chouchane, A., Ouamane, A., Bourennane, S. (2016). Local descriptors and tensor local preserving projection in face recognition.

[31] Hyvarinen, A., et al. (2009). Natural Image Statistics. *Springer*.

[32] Kannala, J., & Rahtu, E. (2012). BSIF: Binarized statistical image features. *Proceedings of the 21st International Conference on Pattern Recognition (ICPR2012)*, 1363-1366.

[33] Danny, T. Biometric System Architecture: Getting Down the Core. *Bayometric*. Retrieved from https://www.bayometric.com/biometric-system-architecture/#:~:text=Biometric%20system%20architecture%20is%20the,human%20interaction%20with%20these%20components

[34] ColorFERET Face Database. Retrieved from https://www.nist.gov/itl/products-and-services/color-feret-database

[35] FEI Face Database. Retrieved from https://fei.edu.br/~cet/facedatabase.html

[36] Tongji Contactless Palmprint Database. Retrieved from https://github.com/AngeloUNIMI/PalmNet/tree/master/images/Tongji_Contactless_Palmprint_Dataset

[37] COEP Palmprint Database. Retrieved from https://www.coep.org.in/resources/coeppalmprintdatabase